Cement & Concrete Composites 33 (2011) 1009–1013

Contents lists available at SciVerse ScienceDirect

Cement & Concrete Composites

journal homepage: www.elsevier.com/locate/cemconcomp

Experimental study of water flow behaviour in narrow fractures of cementitious materials

Kefei Li *, Mingjun Ma, Xiaomei Wang

Key Laboratory of Civil Engineering Safety and Durability of China Education Ministry, Civil Engineering Department, Tsinghua University, 100084 Beijing, PR China

ARTICLE INFO

Article history:
Received 4 March 2010
Received in revised form 11 May 2011
Accepted 17 August 2011
Available online 30 August 2011

Keywords:
Fracture
Roughness
Permeability
Mortar
Concrete

ABSTRACT

This paper reports an experimental investigation on water flow behaviour in narrow fractures of cementitious materials. A permeation device was developed especially for water flow in fractures. Five cementitious materials were retained, specimens were prepared in disk form and fractures were obtained by splitting specimens in three-point bending mode. The topography of fractured surfaces of specimens was scanned by laser profilometer and the surface roughness was quantified by 3D fractal dimension analysis. The fractured specimens were then closed and mounted into the permeation device for flow test by deionized water during 48 h. Furthermore, repetitive flow tests were performed on one fractured specimen to study the sealing effect of fractures. It is observed that the geometrical opening aperture in fractures is very different from the hydraulic equivalent value and the sealing effect of narrow fractures can be mainly attributed to the non-Darcian characteristic of liquid flow between rough surfaces under low pressure gradient.

1. Introduction

Cementitious materials are quasi-brittle in hardened state, liable to cracking under mechanical loadings. During hardening cementitious materials undergo also intrinsic, drying and thermal shrinkages, capable to induce early-age cracking [1,2]. Hence, structural cementitious materials usually contain cracking of different natures during their service lives [3]. For some specific engineering applications such as radioactive waste disposals, cementitious materials serve as engineered barrier against migration of hazardous matters, thus water permeability is identified as the key parameter for structural design [4,5]. In these cases, the role of cracking on permeation-related transport processes has to be quantified. Accordingly, the research on transport process in fractured cementitious materials has been highlighted and recent results can be found in Refs. [6,7]. The experimental aspect of the research on transport properties of cracked concrete is extensively reviewed in Ref. [8]. The existence of cracking turns materials from continuous media to discrete ones thus the involved transport processes can be radically different [9,10]. For cementitious materials, the fractured surface can be moreover chemically active. From the state-of-art of knowledge, key aspects on water transport involve at least water flow behaviour in rough fractures and mass exchange processes between the flowing water and the reactive fracture surfaces [11,12]. Although the control factors for water flow in fractures are well identified as fracture opening, surface roughness as well as surface hydro-reactivity, some fundamental aspects still remain to be explored: how water flow behaviour is correlated to fracture surface properties and how/why water flow rate evolves with time.

This paper attempts to gain some insight on these questions through experimental investigation. Several cementitious materials are retained in this study and fractured specimens were prepared. Then the topography of fracture surfaces of specimens was scanned and the surface roughness is quantified by the fractal dimension. Afterwards, the fractured specimens were subjected to flow test by water and alcohol. The flow behaviour of liquids, water and alcohol, in narrow fractures is analyzed in depth on the basis of the obtained results.

2. Experimental procedure

2.1. Materials and specimens

Five cementitious materials were prepared: one cement paste, three mortars and one concrete, detailed proportioning given in Table 1. The used cement was of type PO42.5 (Portland ordinary cement with nominal strength of 42.5 MPa) according to Chinese cement standard [13], equivalent to CEM II/A type in European Standard [14]. Two sands were used for mortars: fine sand (modulus 1.8) and standard sand (modulus 2.5). The materials were mixed and poured into PVC tubes with inner diameter of 10 cm. After 7 days of standard curing (temperature 20 °C and humidity above 95%), disks with thickness of 3 cm were sawed out and an indent of

* Corresponding author. Tel./fax: +86 10 6278 1408.
E-mail address: likefei@tsinghua.edu.cn (K. Li).

0958-9465/$ - see front matter © 2011 Elsevier Ltd. All rights reserved.
doi:10.1016/j.cemconcomp.2011.08.005

Table 1
Mix proportioning of cementitious materials.

Composition	C1	C2	C3	C4	C5
Cement PO42.5 (kg/m^3)	1385	503	537	503	503
Water (kg/m^3)	553	302	268	302	302
Water to cement ratio (–)	0.40	0.60	0.50	0.60	0.60
Fine sand (kg/m^3) (<5 mm, modulus 1.8)	–	1395	–	–	–
Standard sand (kg/m^3) (<5 mm, modulus 2.5)	–	–	1395	1395	837
Crushed rock (5–15 mm) (kg/m^3)	–	–	–	–	558

5 mm was sawed diametrically on one surface of disk. Then the disks were put again into standard curing conditions till age of 28 days. Then the indented disks were split by three-point bending. To screen the possible surface secondary reaction, all fractured disks were put into water for 2 weeks after splitting. Afterwards, all fractured surfaces were subjected to topography scan and flow tests.

2.2. Permeation device and tests

The experimental device was designed by the authors especially for flow in fractures, the device scheme illustrated in Fig. 1a. The permeation cell of this device is consisted of: the fractured specimen (two parts), a rubber coat for specimen and a mechanical ring outside the rubber coat, cf. Fig. 1b. In the first phase of flow tests, fractured specimens (C1–C5) were mounted into the permeation cell and the mechanical ring was fastened mechanically with the lateral screws. Flow tests were performed under a constant water head of 1.8 m with deionized water as infiltrating liquid. For each fractured specimen, the flow test last for 48 h and the water flow volume and flow rate were recorded. In the second phase, specimen C4 was re-mounted into permeation cell and repetitive flow tests were performed for four cycles: in each cycle water flow test took 36 h and the fractured specimen was dried in permeation cell for 12 h in room condition. Afterwards, a final flow test was conducted on C4 with alcohol as infiltrating liquid. Again, the flow volume and flow rate of liquids (water, alcohol) were recorded.

3. Surface roughness and fracture opening

3.1. Surface roughness quantification

The topography of fractured surfaces was scanned by a large-scale laser profilometer originally designed for surface analysis of rock fractures [15]. The vertical topography scanning precision was ±7 μm with a measuring range of 30 mm. For the fracture surfaces in this study, the effective area for scan was about 2.5 cm × 10 cm, and the topography scanning mesh was 144 lines along long side and 1032 lines along short side. For illustration, the reconstructed fracture surfaces of C1 and C5 are presented in Fig. 2. On the basis of topography data, fractal dimension was selected to characterize the surface roughness. The pertinence of fractal dimension to surface roughness characterization of cementitious materials has been explored [16]. Several methods are available for fractal dimension evaluation while the cubic covering method was retained for this study, detailed algorithm see [15]. With this method the surface roughness is calculated and presented in Table 2. As expected, Specimens C1–C5 give an increasing order for surface roughness due to their aggregate size and water to cement ratio, which agrees with the available surface roughness analysis on cementitious surfaces [17].

3.2. Fracture opening analysis

In this study, the two opposite parts of fractured specimen were re-closed and fastened tightly in permeation cell. If the two opposite surfaces were perfectly complementary one to the other, the fracture opening would be zero and no liquid could pass the fracture. As it can be seen later, all specimens have water flow, i.e. the two opposite surfaces of one fractured specimen cannot be closed completely. The fracture opening analysis is performed in this context for the specimens in permeation cell. Instead of direct observation, a geometrical method is used in this study: for two matched surfaces, one representative profile is extracted from one surface and the corresponding profile at the opposite surface is also extracted; afterwards the two profiles are approached until a geometrical closest state is achieved, i.e. at least two common points come into contact; then the fracture opening aperture is evaluated by the relative position of two profiles at this state. Following this approach, the middle profiles along short side for each specimen are retained for fracture opening analysis and statistic analysis is performed on the available fracture opening values. In Table 2 are presented the average opening, opening deviation and total opening area for each specimen. The profiles' closest state and opening distribution are given in Fig. 3 for Specimen C1. The correlation between surface roughness and fracture opening is presented in Fig. 4.

4. Flow in fractures

4.1. Flow rate in different fractures

The water flow rates of C1–C5 are presented in Fig. 5 with the initial values given in Table 2. The flow rate is calculated from the

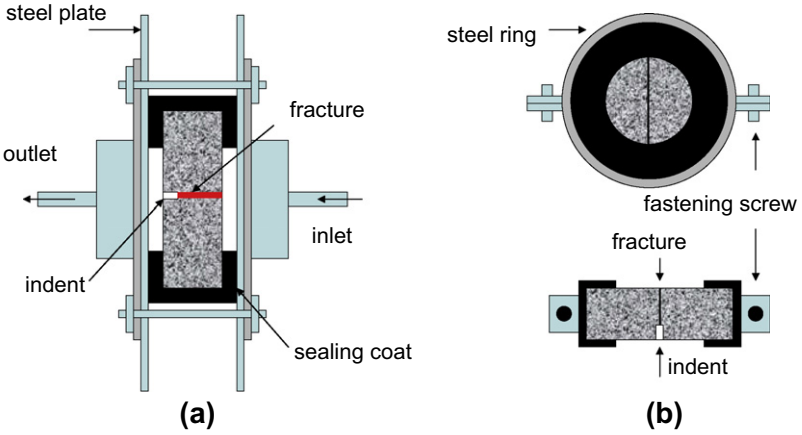

Fig. 1. Experimental device for flow tests (a) and permeation cell for fractured specimens (b).

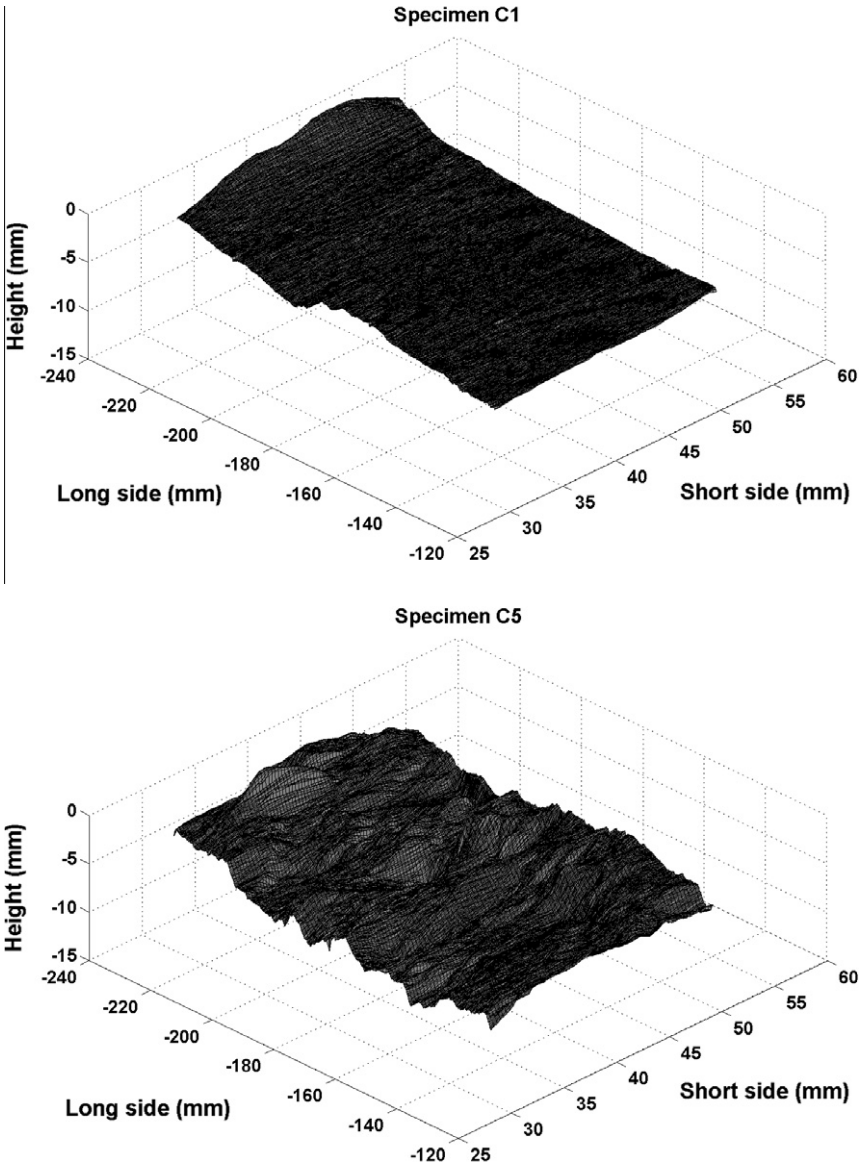

Fig. 2. Scanned rough surfaces of C1 and C5.

recorded flow volume and the average flow rate during the first hour was taken as initial flow rate. From the figure, it can be seen that (1) fractures of rougher surfaces give larger initial flow rates; (2) all flow rates decrease rapidly with time with final rates at 48 h representing 5–10% of their initial values. The equivalent hydraulic opening of fractures can be deduced from the measured initial flow rates through Poiseuille's law for laminar flow [18]:

$$w_e = \sqrt[3]{12\frac{q_0\eta\Delta d}{b\Delta p}} \tag{1}$$

with q_0 for initial flow rate (m^3/s), b for fracture length perpendicular to flow direction (m), w_e for equivalent hydraulic opening of fracture (m), η for water absolute viscosity (Pa s), Δp for water pressure gradient (Pa) and Δd for flow path length in fracture (m). In this study, Δp = 18 kPa, b = 10 cm, Δd = 2.5 cm and η = 0.001 Pa s, the equivalent hydraulic opening is calculated for C1–C5 and given in Table 2.

For the results in Table 2, a first observation is that the equivalent opening is one order less than the geometrical opening and rougher surfaces generate larger geometrical openings as well as equivalent openings. Then the influence of surface roughness on initial flow rates is somehow against common sense: rougher surface provides more friction to water flow thus smaller flow rate should have been observed; however larger flow rates were observed for rougher surfaces in Table 2. In fact, two factors interplay

Table 2
Surface and flow properties of fractured specimens.

Properties	C1	C2	C3	C4	C5
Surface fractal dimension, D (–)	2.0273	2.0703	2.0969	2.1110	2.1270
Average fracture opening, w (mm)	0.1394	0.1554	0.2058	0.2182	0.2619
Opening deviation, σ_w (mm)	0.05516	0.06951	0.09624	0.09889	0.1710
Fracture opening area, A_w (mm^2)	3.4886	3.9021	5.16534	5.4793	6.3816
Initial flow rate, q_0 (ml/h)	19.9	46.0	56.5	84.0	153.6
Equivalent hydraulic opening, w_e (mm)	0.01231	0.01627	0.01743	0.01989	0.02432

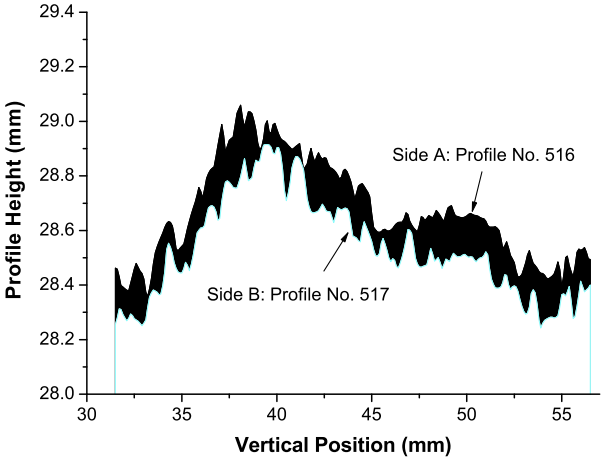

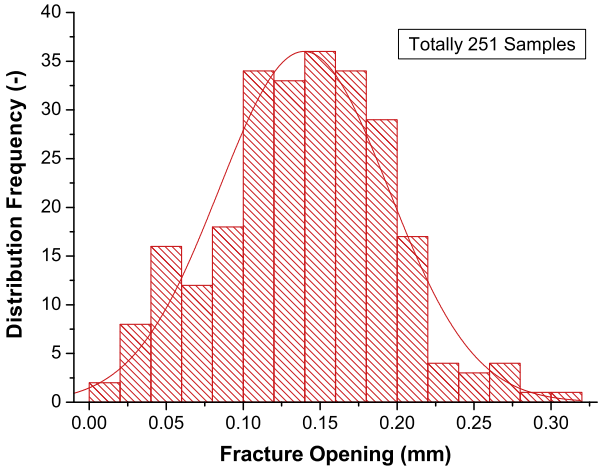

Fig. 3. 2D analysis of fracture opening for Specimen C1.

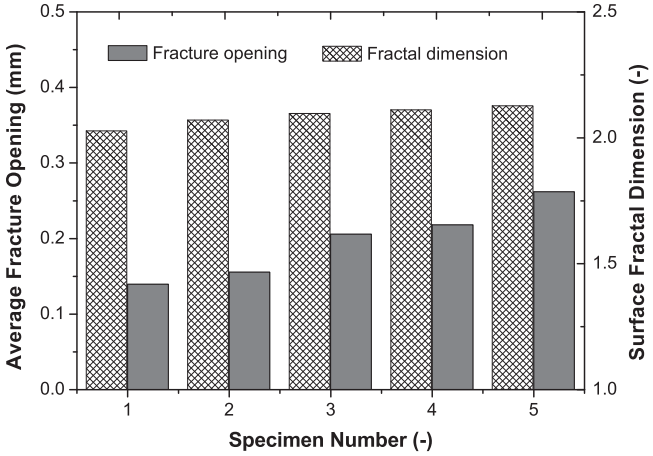

Fig. 4. Analysis on surface roughness and fracture opening apertures.

for water flow across rough surface: surface friction and surface channeling. As observed above, the opposite surfaces of one fracture is not strictly complementary one to the other, and it is due to the irreversible surface deformation associated with the quasi-brittle fracture processes. This leaves surface channels for fracture in its closed state. From the geometrical analysis for opening, one can see that rougher surface has larger residual opening. Through this residual opening water can flow freely, the phenomenon is

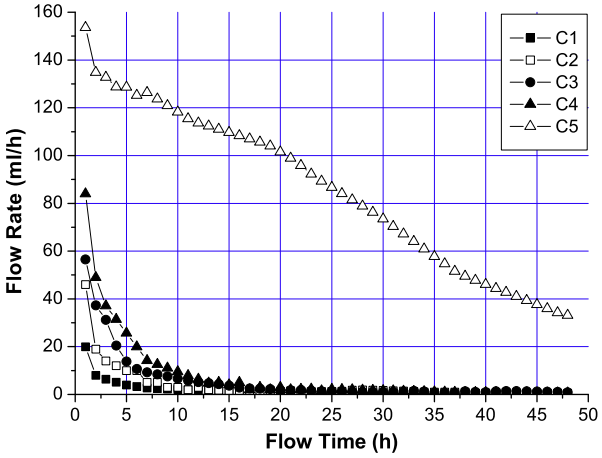

Fig. 5. Flow rates for fractured specimens C1–C5.

named as "surface channeling" in relevant fracture flow literature [19]. From the fact that rougher surfaces give larger flow rates in this study, it can be judged that the contribution of surface channeling to fracture flow dominates over the hindering effect of surface friction on fracture flow. Accordingly, rougher fractures have more important water flow. Certainly, as the opening of fracture surfaces increases from this closed state both surface friction and surface channeling effects are to decrease for liquid flow.

4.2. Repetitive flow rate

The flow rates in repetitive flow tests on C4 are presented in Fig. 6. One can observe: (1) all water flow rates decrease with time as in Fig. 5; (2) the initial flow rates of water decrease with the repetitive cycles; (3) the flow rate by alcohol follows nearly the same decreasing curve as the last water flow rate.

These observations can help to understand some fundamental aspects of the so-called "sealing effect" of fractures. In this study, two sealing effects are evident: the first related to one single flow process and the second associated with the initial flow rates with repetitive cycles. Let us look at the first one. The alcohol, *a priori*, does not react with or dissolve the matter on fractured surfaces, thus the geometry of fracture opening can be regarded as unchanged during the last flow cycle. Accordingly, for alcohol flow the sealing effect of fracture can be purely mechanical. The decreasing flow rate with time is only due to the surface friction and the relatively low flowing pressure while a steady/Darcian flow is expected at a higher pressure. In other words, the flowing pressure, 14.4 kPa for alcohol, is not enough to generate a Darcian flow of alcohol in the narrow fracture of C4, and the transient flow rate is a characteristic of non-Darcian flow. For a single water flow process, the dissolution and possible re-precipitation of $Ca(OH)_2$ in water cannot be excluded [12]. However, considering the very low concentration of CO_2 in deionized water used in this study the dissolution–precipitation process cannot be that important to reduce the initial flow rate to its 5–10% in 36 h. Thus, it can be deduced that the transient rate of water is also an evidence of non-Darcian flow due to the rough surface friction and low flowing pressure (18 kPa for water).

Here comes the second sealing effect with water flow cycles. Taking into account the experimental procedure described above, the fractured surfaces of specimen were subjected alternatively to water flow (36 h) and surface drying (12 h). During flow test water can dissolve $Ca(OH)_2$ on fracture surface while precipitation of $CaCO_3$ can happen with CO_2 in atmosphere during drying. This precipitation happened in every drying period thus reduced the fracture opening for the subsequent water flow.

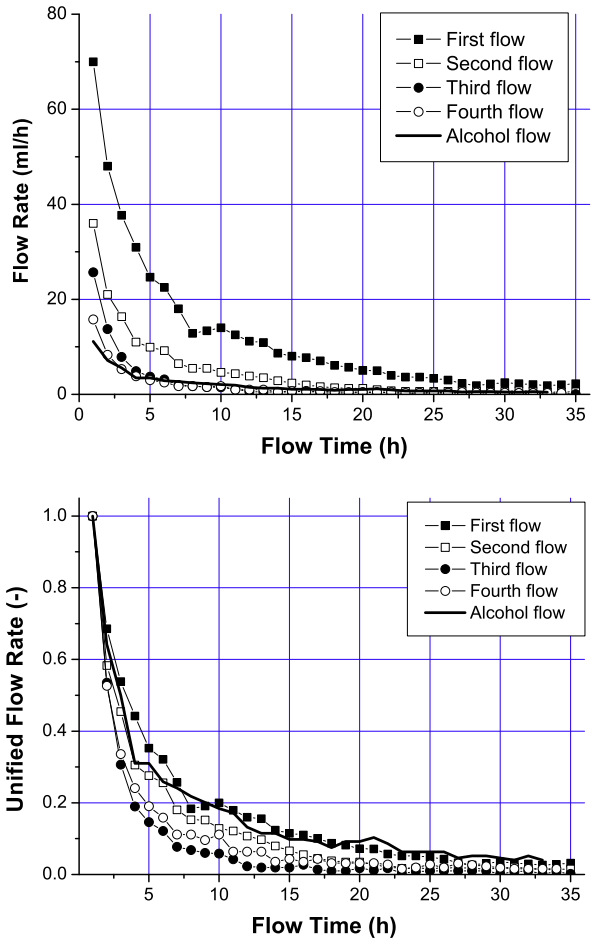

Fig. 6. Absolute and unified flow rates for repetitive flow tests on specimen C4.

5. Concluding remarks

1. Surface roughness of cementitious materials can be represented by fractal dimension. Aggregate size and water to cement ratio are determinant factors for surface roughness. Fracture surfaces of cementitious materials, once formed, cannot be closed completely. The residual opening of fractured surfaces is intimately related to the surface roughness. Rougher surfaces have larger residual opening.
2. Water flow in fractures in this study takes place in the residual fracture opening after the reclosure of fracture surfaces. Surface channeling effect dominates over the surface friction effect so that rougher surfaces have larger (initial) water flow rates. However, the geometrical width of residual fracture opening is one order greater than the equivalent hydraulic opening deduced from Poiseuille's law.
3. Sealing effect of fractures can have two different causes. The mechanical cause is that liquid flow in narrow and rough fractures, under low flow pressure, can assume non-Darcian behaviour with transient flow rate decreasing substantially with time. The chemical cause can be surface dissolution during flow and surface precipitation during drying, which changes the rough surface topography as well as the fracture surface channeling.

Acknowledgements

The research is supported by national Natural Science Foundation of China (NSFC) Grant Nos. 50538060 and 50978144. The help of Mr. Zhang Zhiling in fabrication of permeation cell is acknowledged.

References

[1] Neville AM. Properties of concrete. 4th ed. Harlow: Pearson Education; 1995.
[2] Mehta PK, Monteiro PJM. Concrete microstructure, properties and materials. 3rd ed. New York: McGraw-Hill; 2006.
[3] Burrows RW. The visible and invisible cracking of concrete. ACI monograph No. 11. Farmington Hills: American Concrete Institute; 1998.
[4] International Atomic Energy Agency. Performance of engineered barrier materials in near surface disposal facilities. IAEA-TECDOC-1225. Vienna: IAEA; 2001.
[5] International Atomic Energy Agency. Safety guide: safety assessment for near surface disposal of radioactive waste. IAEA safety standards series No. WS-G-1.1. Vienna: IAEA; 1999.
[6] Breysse D, Gérard B. Transport of fluid in cracked media. In: Reinhardt HW, editor. Penetration and permeability of concrete: barriers to organic and contaminating liquids. RILEM report 16. London: E& FN Spon; 1998.
[7] Audenaert K, Marsavina L, De Shutter G. Transport mechanisms in cracked concrete. Leuven: Uitgeverij Acco; 2007.
[8] Hoseini M, Bindiganavile V, Banthia N. The effect of mechanical stress on permeability of concrete: a review. Cem Concr Compos 2009;31(4):213–20.
[9] Neuman SP. Trends, prospects and challenges in quantifying flow and transport through fractured rocks. Hydrogeol J 2005;13(1):127–47.
[10] Dai JG, Akira Y, Wittmann FH, Yokota H, Zhang P. Water repellent surface impregnation for extension of service life of reinforced concrete structures in marine environments: the role of cracks. Cem Concr Compos 2010;32(2):101–9.
[11] Drazer G, Koplik J. Permeability of self-affine rough fractures. Phys Rev E 2000;62(6):8076–85.
[12] Edvardsen C. Water permeability and autogenous sealing of cracks in concrete. ACI Mater J 1999;96(4):448–54.
[13] Chinese Cement Standard. Common portland cement (GB175-2007). Beijing: Chinese Standard Publishing; 2007.
[14] European Standard. Cement. Part 1: Composition, specifications and conformity criteria for common cements. Brussels: European Committee for Standadization; 2000.
[15] Zhou HW, Xie H. Direct estimation of the fractal dimension of a fracture surface of rock. Surf Rev Lett 2003;10(5):751–62.
[16] Winslow D. The fractal nature of the surface of cement paste. Cem Concr Res 1985;15(5):817–24.
[17] Mohsen Issa A, Mahmoud Issa A, Islam SMd, Chudnovsky A. Fractal dimension – a measurement of fracture roughness and toughness of concrete. Eng Fract Mech 2003;70(1):125–37.
[18] Streeter VL, Wylie EB, Bedford KW. Fluid mechanics. 9th ed. Beijing: Tsinghua University Press; 2003.
[19] Meheust Y, Schmittbuhl J. Scale effects related to flow in rough fractures. Pure Appl Geophys 2003;160(5):1023–50.